Author Manuscript

Author Manuscript

Author Manuscript

Author Manuscript

HHS Public Access

Author manuscript

Radiother Oncol. Author manuscript; available in PMC 2019 April 01.

Published in final edited form as:

Radiother Oncol. 2018 April ; 127(1): 128–135. doi:10.1016/j.radonc.2018.02.011.

4π plan optimization for cortical-sparing brain radiotherapy

Vyacheslav L. Murzin, Ph.D.[1], **Kaley Woods, B.S.**[2], **Vitali Moiseenko, Ph.D.**[1], **Roshan Karunamuni, Ph.D.**[1], **Kathryn R. Tringale, MAS**[1], **Tyler M. Seibert, M.D., Ph.D.**[1], **Michael J. Connor, B.S.**[3], **Daniel R. Simpson, M.D.**[1], **Ke Sheng, Ph.D.**[2], and **Jona A. Hattangadi-Gluth, M.D.**[1,*]

[1]Department of Radiation Medicine and Applied Sciences, University of California San Diego, La Jolla, CA 92093

[2]Department of Radiation Oncology, University of California Los Angeles, Los Angeles, CA 90095

[3]University of California Irvine School of Medicine, Irvine, CA 92617

Abstract

Background and Purpose—Incidental irradiation of normal brain tissue during radiotherapy is linked to cognitive decline, and may be mediated by damage to healthy cortex. Non-coplanar techniques may be used for cortical sparing. We compared normal brain sparing and probability of cortical atrophy using 4π radiation therapy planning vs. standard fixed gantry intensity-modulated radiotherapy (IMRT).

Material and Methods—Plans from previously irradiated brain tumor patients ("original IMRT", n=13) were re-planned to spare cortex using both 4π optimization ("4π") and IMRT optimization ("optimized IMRT"). Homogeneity index (HI), gradient measure, doses to cortex and white matter (excluding tumor), brainstem, optics, and hippocampus were compared with matching PTV coverage. Probability of three grades of post-treatment cortical atrophy was modeled based on previously established dose response curves.

Results—With matching PTV coverage, 4π significantly improved HI by 27% (p=0.005) and gradient measure by 8% (p=0.001) compared with optimized IMRT. 4π optimization reduced mean and equivalent uniform doses (EUD) to all standard OARs, with 14–15% reduction in hippocampal EUD (p≤0.003) compared with the other two plans. 4π significantly reduced dose to fractional cortical volumes (V_{50}, V_{40} and V_{30}) compared with the original IMRT plans, and reduced cortical V_{30} by 7% (p=0.008) compared with optimized IMRT. White matter EUD, mean dose, and fractional volumes V_{50}, V_{40} and V_{30} were also significantly lower with 4π (p≤0.001). With 4π, probability of grade 1, 2 and 3 cortical atrophy decreased by 12%, 21% and 26% compared with original IMRT and by 8%, 14% and 3% compared with optimized IMRT, respectively (p≤0.001).

[*]**Corresponding Author:** Jona A. Hattangadi-Gluth, MD, Department of Radiation Medicine and Applied Sciences, 3855 Health Sciences Drive, La Jolla, CA 92093, jhattangadi@ucsd.edu, (858) 822-6040/(858) 246-1505 (fax).

Publisher's Disclaimer: This is a PDF file of an unedited manuscript that has been accepted for publication. As a service to our customers we are providing this early version of the manuscript. The manuscript will undergo copyediting, typesetting, and review of the resulting proof before it is published in its final citable form. Please note that during the production process errors may be discovered which could affect the content, and all legal disclaimers that apply to the journal pertain.

Author Manuscript Author Manuscript Author Manuscript Author Manuscript

Conclusions—4π radiotherapy significantly improved cortical sparing and reduced doses to standard brain OARs, white matter, and the hippocampus. This was achieved with superior PTV dose homogeneity. Such sparing could reduce the probability of cortical atrophy that may lead to cognitive decline.

Keywords

Intracranial radiotherapy; Non-coplanar IMRT; brain sparing; NTCP; cortical atrophy

Introduction

Radiation therapy (RT) is a mainstay in the treatment of brain tumors, but incidental irradiation of normal brain tissue beyond the tumor is unavoidable. This has been linked to late effects on cognitive function [1–5]. As brain tumor patients survive longer [6,7], treatment-related neurocognitive decline is becoming increasingly important [7]. Technological advances in radiotherapy, e.g., use of intensity-modulated radiotherapy (IMRT), volumetric modulated arc therapy (VMAT) [8] and image guidance [9], provide a means to deliver radiotherapy in a more conformal and accurate manner. Use of non-coplanar IMRT fields or arcs adds extra degrees of freedom in shaping dose distribution [10]. Region-specific and whole-brain sparing planning studies show potential benefits of optimizing radiation delivery pathways [10,11]. More recently, there has been increased attention to a new radiation therapy planning technique called 4π IMRT, which can significantly reduce dose to normal tissues via optimization of non-coplanar beam angles [12–14].

The QUANTEC group (quantitative analysis of normal tissue effects in the clinic) publishes guidelines for normal tissue sparing [15], yet notes a lack of high-level evidence for brain treatment [16]. While recommendations to avoid symptomatic necrosis are provided, constraints to preserve cognitive performance are not well defined. Creating such parameters requires careful consideration of neuroanatomic regions in the context of their sensitivity to radiotherapy and their role in cognitive functioning.

Normal-appearing cerebral cortex beyond the tumor/target exhibits dose-dependent atrophy after brain radiotherapy which parallels neurodegenerative diseases [17]. Areas of cortex which are critical for higher-order cognition appear to be most vulnerable to radiation-related atrophy [18]. In studies of aging and degenerative diseases, cortical atrophy is associated with cognitive dysfunction [19–22]. Other studies have reported dose-dependent changes in white matter after radiation therapy using diffusion tensor imaging [23–25], and these biomarkers of white matter injury are correlated with decline in neurocognitive functioning [26,27]. Lately there has been an increased focus on the role of the hippocampus in mediating radiation-induced neurocognitive decline [28–30], and a recent study reports dose-dependent hippocampal atrophy after brain tumor radiotherapy [31]. While non-coplanar IMRT and VMAT can improve the ability to spare normal brain, the optimal method for sparing critical brain structures, especially those with relevance to cognition, is unclear.

Author Manuscript Author Manuscript Author Manuscript Author Manuscript

A recent study established radiation treatment planning objectives for brain cortex [32], showing the feasibility of cortical-sparing with optimized IMRT/VMAT. However, heavily prioritizing cortical dose in standard IMRT optimization was shown to compromise other aspects of the plans including PTV dose homogeneity. We sought to analyze whether novel 4π-IMRT planning could improve cortical sparing as well as the overall plan quality. We first compare original standard-of-care IMRT plans, cortical sparing-optimized IMRT plans, and 4π-optimized plans. Next, we model the probability of developing cortical atrophy among the planning techniques based on cortical doses in a normal tissue complication probability model [32]. We hypothesized that 4π optimization would allow better sparing of cortical volumes and that this would translate to an improvement in the probability of dose-dependent cortical atrophy.

Materials and Methods

Patient Population and Treatment

This retrospective study was approved by the institutional review board. The patient cohort consisted of 9 male and 4 female subjects (median age 60 years, range 40–77) with high grade glioma. Patients were treated on a 6MV TrueBeam (Varian Medical Systems, Palo Alto, CA) linear accelerator with a 120-leaf Millennium multi-leaf collimator to a prescription dose of 59.4Gy (N=1) and 60Gy (N=12) in 33 or 30 fractions, respectively. All patients original clinical plans were 6–8 non-coplanar field, fixed-gantry, sliding-window IMRT. The original IMRT plans were obtained and re-planned with region-specific cortical-sparing IMRT optimization [32], and 4π radiation therapy optimization.

MRI Imaging and Segmentation

In each case, MR imaging was performed on a 3T Signa Excite HDx scanner (GE Healthcare, Milwaukee, Wisconsin) equipped with an 8-channel head coil. The imaging protocol included pre- and post contrast 3D volumetric T1-weighted inversion recovery spoiled gradient-echo sequence (TE, 2.8 ms; TR, 6.5 ms; TI, 450 ms) and a 3D T2-weighted FLAIR sequence (TE, 126 ms; TR, 6000 ms; TI,1863 ms). As previously described, all MR images were corrected for geometric distortions due to susceptibility, gradient nonlinearities, and eddy currents [32]. Cortical volumes, subcortical white matter and hippocampus were segmented using Freesurfer (version 5.3; available at http://surfer.ndm.harvard.edu), as previously described [17,32]. Surgical scar, tumor, tumor beds and resection cavities were manually censored from analyses since these areas do not contain viable normal tissue for sparing. Cortex, subcortical white matter, and hippocampus were imported into the research Eclipse™ treatment planning system (Varian Medical Systems, Palo Alto, CA) for re-planning. Contours were visually inspected to ensure that all volumes were properly segmented. Cortical, hippocampal, and white matter segmentations were processed to remove regions that overlapped with the planning target volume (PTV) since these areas are not viable for OAR sparing.

Radiation planning objectives

The original fixed gantry IMRT plans were optimized to meet clinical objectives for PTV coverage and standard OARs (including brainstem, optic structures, and spinal cord) at the

Author Manuscript Author Manuscript Author Manuscript Author Manuscript

time when treatment was administered. Dose constraints matched guidelines set by RTOG 0825 [33], including max doses of brainstem <60Gy, optic nerves <55Gy and optic chiasm <56Gy. Field arrangements for these plans were selected by the treating physician and dosimetry team to most effectively achieve planning goals for each case. These original clinical plans were not optimized for cortical sparing. For each case, two cortical-sparing replans were performed: IMRT-optimized and 4π-optimized. Cortical sparing for the IMRT-optimized plans was performed to minimize cortical volume outside the PTV receiving higher than 30Gy [32], with the highest priority given to the cortex. In 4π planning the highest constraint for each case was also placed on the normal cortex, then the other OARs prioritized based on proximity of OARs to tumor.. The overarching goal was to minimize OAR doses while matching the primary objective for PTV coverage in the original plan. The objectives and priorities used for the cortical sparing IMRT plans and cortical sparing 4pi plans were the same, and were prioritized the same way. Doses in all plans were normalized so that 100% of the prescription dose covered 95% of the PTV volume.

4π optimization

The 4π treatment planning process is a highly non-coplanar and non-isocentric system developed on C-arm gantry linear accelerators, and has been described in detail previously [12–14,34]. Briefly, 4π planning began with 1162 candidate beams evenly distributed throughout the solid sphere angle space, with 6° separation between beams. A computer-aided design (CAD) model of the Varian TrueBeam linear accelerator with a 3D scanned human surface model positioned on the couch was utilized to exclude any beams causing a collision between the gantry and couch or patient [45]. Dose contribution matrices with 2.5 × 2.5 × 2.5 mm^2 resolution were computed for each of the candidate beams using convolution/superposition of a 6MV polyenergetic X-ray kernel. A greedy column generation algorithm, with defined upper dose constraints and structure priority weightings, was used to iteratively select 20 beam orientations and perform fluence map optimization [35]. To compare with the clinical plans without any bias from different dose calculation methods, the optimal beam orientations were then imported into Eclipse for dose recalculation using an identical dose calculation engine and resolution.

Dosimetric comparison of the plans (PTV and OARs)

Dosimetric parameters for PTV and OARs from each of the three plans were evaluated including maximum point dose, mean dose and equivalent uniform doses (EUD). For the latter the generalized EUD formalism was used [36]: $EUD = \left(\frac{\sum_{i=1}^{N} D^a}{N} \right)^{\frac{1}{a}}$, where the value of the parameter a signifies sensitivity to cold spots for tumors and hot spots for normal tissues. For brain tissues a=5; brainstem a=7; optic chiasm, optic nerves, cochlea a=25; and for tumor a= −10 [37].

Furthermore, OAR fractional volumes V_X receiving at least dose X (X = 60, 50, 40 and 30 Gy) were calculated and included in the comparison.

Author Manuscript Author Manuscript Author Manuscript Author Manuscript

The PTV conformity index (CI) and homogeneity index (HI) were calculated to test for spillage of the prescription dose outside of PTV and hot/cold spots inside PTV. CI was defined as the ratio of the volume receiving the prescribed dose to the volume of the PTV: $CI = \frac{V_P}{V_{PTV}}$ and homogeneity index as $HI = \frac{D_2 - D_{98}}{D_P} \cdot 100\%$, where D_2 and D_{98} are minimum doses for 2% and 98% of PTV assessed from the cumulative DVH, and D_P is the prescribed dose [38,39]. Gradient measure is defined as the difference in radius of equivalent sphere of the prescription and 50% isodose lines, measured in centimeters.

NTCP modeling of cortical atrophy

Probability of developing radiation-induced cortical atrophy was modeled using the logistic function:

$$p = \frac{1}{1 + e^{-4\gamma_{50}\left(\frac{D}{D_{50}} - 1\right)}},$$

where D_{50} is the dose that results in 50% chance of developing complication and γ_{50} is the normalized slope of the NTCP curve at the dose D_{50}. Model parameter values used in our calculations were previously reported [32] with grades of complication assigned according to the extent of cortical thinning at 1 year post-RT: >2% grade 1 (γ_{50}=0.29, D_{50} =16.88), >3% grade 2 (0.62, 29.78) and >5% grade 3 (1.24, 39.77). To facilitate a comparison of 3D volume per voxel probability of cortical thinning, we chose to use a mean probability of cortical thinning given that this probability is directly correlated to dose. Mean probability of developing complication (proportion of voxels exhibiting cortical thinning) was estimated as an arithmetic mean of the probabilities for each voxel $p_{mean} = \frac{\sum_{i=1}^{N} p_i}{N}$.

Statistical Analysis

Changes in the treatment plan statistical averages were compared using Wilcoxon matched-pairs signed-rank test. Differences between plans were considered statistically significant for $p<0.005$ (after Bonferroni correction for 10 independent tests). Primary endpoints in the analysis were: gradient measure, conformity and homogeneity indices and doses to OARs (cortex outside PTV, white matter outside PTV, brainstem, optic chiasm, ipsilateral and contralateral optic nerves and hippocampus, Figure 1). As an ad-hoc analysis, we also assessed whether tumor location or PTV size predicted for the difference in probability of grade 3 cortical atrophy between the treatment plans. All statistical tests were two-sided and all calculations were performed in Matlab (Mathworks, Natick, MA).

Results

Dosimetric comparison of the plans is summarized in Table 1. This comparison included independent tests (primary endpoints) and tests based on biological response assumptions (EUD, NTCP of cortical thinning) and 4π was tested against both clinical (IMRT original) plans and IMRT plans optimized for cortical sparing (IMRT optimized). 4π and IMRT

Author Manuscript Author Manuscript Author Manuscript Author Manuscript

optimized planning provided comparable PTV coverage, with slightly higher (+2%, p=0.001) conformity index (CI) for 4pi plans compared with original clinical. The homogeneity index of 4π was significantly lower than optimized IMRT (−27%, p=0.005), and comparable to the original clinical plans. With 4π, gradient measure was reduced by 20% (p<0.001) compared with the original plans and by 8% compared with optimized IMRT (p=0.001), indicating that 4π achieves faster dose fall off outside of the PTV.

Dose-volume histogram (DVH) analysis (example shown in Figure 2) showed that 4π planning reduced overall doses to all brain OARs. With 4π, mean doses to cerebral cortex excluding PTV decreased by 25% (p<0.001), to hippocampus by 38% (p=0.002) and to white matter excluding PTV by 23% (p<0.001) compared to original plans. Mean cortical and white matter doses were significantly lower with 4π compared with optimized IMRT, along with mean dose to ipsilateral optic nerve and chiasm, Table 1. Relative change in EUD to OARs among the three plans are shown in Figure 3, with patients sorted on x-axis by the dose in original plan. Compared with clinical plans, 4π reduced EUD to normal cortex and white matter in all patients. Compared with optimized IMRT, 4π planning did not significantly change cortical EUD, but the median values of white matter EUD (−5%, p=0.001) and hippocampal EUD (−15%, p=0.001) were significantly lower along with a 45% reduction in brainstem EUD (p=0.001).

Changes in fractional volume receiving 60Gy or more, V_{60}, were not significant among the three plans. Comparing 4π and clinical plans, V_{30}, V_{40} and V_{50} decreased by 11–38% for cortex and 23–31% for white matter, Table 1. Comparing 4π and optimized IMRT plans, white matter V_{30} and V_{40} were significantly lower with 4π, and cortical V_{30} was 7% lower though this did not meet our pre-determined threshold for statistical significance (p=0.008). Example of the dose distribution on cortical surface minus PTV for both plans is shown in Figures 4a and 4b and the map of the absolute difference in Figure 4c.

Probability of cortical thinning using NTCP was calculated on dose per-voxel basis. When averaged across voxels, this probability can be viewed as proportion of voxels that are estimated to experience a given degree of cortical thinning. The probability of cortical atrophy by grade (median and range) is shown in Table 1. 4π planning significantly reduced the probability of each grade of cortical atrophy when compared with standard clinical and optimized IMRT plans.

Median PTV size was 90.1 cc (range 17.7 cc–188.9 cc). As PTV volume increases, the difference in probability of developing grade 3 (>5%) cortical atrophy with 4π versus the standard clinical plan (probability with 4π planning minus probability with original clinical plan) decreased (−0.83, p=0.0004, Pearson's correlation coefficient); this indicates a greater decrease in probability of atrophy with 4π optimization with larger PTVs. Tumor location (analyzed as temporal location vs. non-temporal) was not associated (p=0.07, Mann-whitney Wilcoxon test) with the difference in probability of atrophy between 4π and the other treatment plans.

Cochlear doses are shown in supplementary Table 1. There was no difference in dose to ipsilateral or contralateral cochlea between the plans.

Author Manuscript Author Manuscript Author Manuscript Author Manuscript

Discussion

Reducing the volume of incidentally irradiated normal brain structures in brain RT may help to lower the probability of cortical, white matter, and hippocampal damage that could lead to late neurocognitive deficits. A previous study showed that cortical sparing was feasible by heavily prioritizing cortical dose in standard IMRT planning [32]. This leads to two follow-up questions: First, can cortical dose be further reduced using new planning methods? Second, can improved cortical sparing be achieved without compromising other planning metrics including PTV dose homogeneity? In this study, standard-of-care original and optimized IMRT plans were compared to 4π-optimized IMRT plans. 4π improved sparing of all standard OARs including brainstem and optic structures. Our results also show that 4π radiation therapy would reduce V_{30} by 38% for normal cortex and 31% for white matter ($p<0.001$) when compared to original IMRT. Since doses over 30Gy increase (20% or greater) probability of severe cortical thinning [32], 4π optimized IMRT has the potential to lower cortical injury.

Plans optimized for region-specific cortical sparing also reduce V_{30} as previously shown [32] but these doses can be further 4π-optimized by 7% ($p=0.008$) for cortex and by 20% ($p<0.001$) for white matter. These effects may have potential to decrease the burden of neuro-cognitive injury. Biomarkers of white matter damage measured with diffusion tensor imaging are highly dose-dependent [25,40], with injury occurring even at low doses [25]. In WBRT patients, dose to the hippocampus is postulated to mediate post-treatment decline in verbal memory [41] and a recent quantitative MRI study reported dose-dependent hippocampal atrophy [31] after brain RT. Notably, even though none of the plans were optimized with respect to the hippocampus, 4π-optimized IMRT significantly reduced mean dose to the hippocampus by 38–39% compared with both original and optimized IMRT, suggesting this technique would be helpful in hippocampal avoidance. Also, while cortical sparing in optimized IMRT was achieved at the price of increased inhomogeneity of PTV coverage [32], 4π optimization allows for better cortical sparing without significant increase in inhomogeneity. The reduced dose to the hippocampus and white matter with 4pi optimized to cortical sparing appears to be an additional benefit of limiting dose-spill outside the PTV.

To our knowledge, this is the first study to estimate the impact of 4π radiotherapy on normal tissue complication probability in brain radiotherapy, namely probability of cortical thinning. 4π radiotherapy has been previously demonstrated to significantly reduce mean/maximum doses in the planning studies for head and neck tumors [14,42], lung and liver [12,13,34,43] and prostate [44]. These studies showed that 4π planning reduces dose spillage volume and dose gradient, maximum and mean doses to proximal OARs while satisfying prescription objectives. In addition, 4π allows for escalation of maximum doses to PTV without significant impact on OARs [42]. Other studies have shown that optimized non-coplanar VMAT trajectories can improve OAR sparing and reduce NTCP [10].

Not all patients are expected to benefit from this new technique to the same degree. This study focused on glioma patients and while overall results are convincing, a broad variation in dosimetric benefits was observed. We found that the benefit of 4π optimization, when

Author Manuscript Author Manuscript Author Manuscript Author Manuscript

compared with standard clinical IMRT plans, appeared to be greater with larger PTV size. With larger volumes and greater “dose spill” with standard VMAT/IMRT treatment, there are likely greater cortical volumes at risk for doses in excess of 30Gy which lead to cortical thinning. In such cases, 4π optimization to improve cortical sparing would have a greater impact on decreasing the probability of cortical atrophy. We were not powered to evaluate the impact of tumor location on the benefit of this technique, but given that cortical volumes are throughout the brain (unlike the hippocampus, for example, which resides in the medial temporal lobe), we would not expect tumor location to make a difference. Systematically studying factors influencing the potential benefit of 4π optimization, in particular tumor size and location, will require a substantially larger cohort with variations in tumor characteristics sufficient for stratification. Also, a planning comparison of 4π against multiple non-coplanar VMAT for intracranial SRS will be a natural next step for considering its use in intracranial RT. Brain tumor patients with longer life expectancy, including children and young adults, and those with the potential for the greatest gain in normal brain sparing would likely be those for whom 4π optimization may be best-suited.

Implementation of new technology cannot be separated from practical aspects which impact availability, planning time, quality assurance and patient throughput. 4π plans, after being imported to an FDA-approved planning system, can be assessed through quality assurance procedures and delivered as standard clinical plans. The delivery efficiency of 4π is currently under investigation. In a prospective patient trial, it has been observed that manual delivery of 4π including 4 sets of images for brain patients can take up to 50 minutes, but the time was reduced to approximately 32 minutes using remote couch rotation. For non-patient treatment using fully automated delivery, the treatment time can be further reduced to 10 minutes [45], in line with multiple arc VMAT. The feasibility of fully automated delivery has been tested on the Varian TrueBeam by executing XML scripts in the Varian TrueBeam Developer Mode. The adoption of this technique into the clinical workflow is currently limited by FDA approval and pending commercial release, rather than any hardware limitations.

This study showed that further improvement in critical brain tissue sparing is feasible with 4π optimization. Dose reduction in these normal tissues may be critical to decreasing incidence of clinically relevant complications. We recognize that further research is needed to link these dosimetric advantages to a functional advantage in normal tissue sparing, e.g., cortical thinning considered in this study. Studies of this nature are already underway at our institution. Future prospective trials that measure the potential gains of 4π radiotherapy in brain tumor patients are warranted, which should include robust measurements of neurocognitive functioning and imaging biomarkers.

Supplementary Material

Refer to Web version on PubMed Central for supplementary material.

Acknowledgments

Funding

Author Manuscript Author Manuscript Author Manuscript Author Manuscript

This work was partially supported by the following grants: National Institutes of Health (R43CA183390 to K.S. and KL2RR031978; KL2TR00099, UL1TR000100 to J.H-G.; #1TL1TR001443 to K.R.T); American Cancer Society (Pilot Award ACS-IRG #70-002 to J.H-G.); National Cancer Institute Cancer Center (Specialized Grant P30CA023100 to J.H-G.); Varian Medical Systems (to K.S.).

References

1. Meyers CA, Brown PD. Role and relevance of neurocognitive assessment in clinical trials of patients with CNS tumors. J Clin Oncol. 2006; 24:1305–9. DOI: 10.1200/JCO.2005.04.6086 [PubMed: 16525186]
2. Tallet AV, Azria D, Barlesi F, Spano J, Carpentier AF, Gonçalves A, et al. Neurocognitive function impairment after whole brain radiotherapy for brain metastases: actual assessment. 2012:1–8.
3. Greene-schloesser D, Moore E, Robbins ME. Molecular Pathways: Radiation-Induced Cognitive Impairment. 2013; 19:2294–300. DOI: 10.1158/1078-0432.CCR-11-2903
4. McDuff SGR, Taich ZJ, Lawson JD, Sanghvi P, Wong ET, Barker FG, et al. Neurocognitive assessment following whole brain radiation therapy and radiosurgery for patients with cerebral metastases. J Neurol Neurosurg Psychiatry. 2013; 84:1384–91. DOI: 10.1136/jnnp-2013-305166 [PubMed: 23715918]
5. Saad S, Wang TJC. Neurocognitive Deficits After Radiation Therapy for Brain Malignancies. Am J Clin Oncol. 2015; 38:634–40. DOI: 10.1097/COC.0000000000000158 [PubMed: 25503433]
6. Stupp R, Weber DC. The Role of Radio- and Chemotherapy in Glioblastoma. 2005; :315–7. DOI: 10.1159/000085575
7. Lin N, Wefel J, Lee E, Schiff D, van den Bent M, Soffietti R, et al. Response Assessment in Neuro-Oncology. Challenges relating to solid tumour brain metastases in clinical trials, part 2: Neurocognitive, neurological, and quality-of-life outcomes. A report from the rano group. Lancet Oncol. 2013; 14:e407–416. [PubMed: 23993385]
8. Shaffer R, Nichol A, Vollans E, Fong M, Nakano S, Moiseenko V, et al. Clinical and practical considerations for the use of intensity-modulated radiotherapy and image guidance in neuro-oncology. Clin Oncol (R Coll Radiol). 2014; 26:395–406. [PubMed: 24840405]
9. Burnet NG, Jena R, Burton KE, Tudor GSJ, Scaife JE, Harris F, et al. Clinical and Practical Considerations for the Use of Intensity-modulated Radiotherapy and Image Guidance in Neuro-oncology Statement of Search Strategies Used and General Considerations of IMRT for Central Nervous System Tumours. Clin Oncol. 2014; 26:395–406. DOI: 10.1016/j.clon.2014.04.024
10. Smyth G, Evans PM, Bamber JC, Mandeville HC, Welsh LC, Saran FH, et al. Non-coplanar trajectories to improve organ at risk sparing in volumetric modulated arc therapy for primary brain tumors. Radiother Oncol. 2016; :1–8. DOI: 10.1016/j.radonc.2016.07.014
11. Dunlop A, Welsh L, Mcquaid D, Dean J, Gulliford S, Hansen V, et al. Brain-Sparing Methods for IMRT of Head and Neck Cancer. 2015; :1–13. DOI: 10.1371/journal.pone.0120141
12. Dong P, Lee P, Ruan D, Long T, Romeijn E, Low D, et al. 4pi noncoplanar stereotactic body radiation therapy for centrally located or larger lung tumors. Int J Radiat Oncol Biol Phys. 2013; 86:407–13. [PubMed: 23523322]
13. Dong P, Lee P, Ruan D, Long T, Romeijn E, Yang Y, et al. 4pi non-coplanar liver SBRT: A novel delivery technique. Int J Radiat Oncol Biol Phys. 2013; 85:1360–6. [PubMed: 23154076]
14. Rwigema J, Nguyen D, Heron D, Chen A, Lee P, Wang P, et al. 4pi noncoplanar stereotactic body radiation therapy for head-and-neck cancer: Potential to improve tumor control and late toxicity. Int J Radiat Oncol Biol Phys. 2015; 91:401–9. [PubMed: 25482301]
15. Marks LB, Light KL, Hubbs JL, Georgas DL, Jones EL, Wright MC, et al. The Impact of Advanced Technologies on Treatment Deviations in Radiation Treatment Delivery. Int J Radiat Oncol Biol Phys. 2007; 69:1579–86. DOI: 10.1016/j.ijrobp.2007.08.017 [PubMed: 18035214]
16. Lawrence Y, Li X, el Naqa I, Hahn C, Marks L, Merchant T, et al. Radiation dose-volume effects in the brain. Int J Radiat Oncol Biol Phys. 2010; 76:S20–27. [PubMed: 20171513]
17. Karunamuni R, Bartsch H, White NS, Moiseenko V, Carmona R, Marshall DC, et al. Dose-Dependent Cortical Thinning After Partial Brain Irradiation in High-Grade Glioma. Radiat Oncol Biol. 2016; 94:297–304. DOI: 10.1016/j.ijrobp.2015.10.026

Author Manuscript Author Manuscript Author Manuscript Author Manuscript

18. Seibert T, Karunamuni R, Kaifi S, Burkeen J, Connor M, Krishnan A, et al. Cerebral Cortex Regions Selectively Vulnerable to Radiation Dose-Dependent Atrophy. Int J Radiat Oncol Biol Phys2. 2017; 97:910–8.
19. Sabuncu MR, Desikan RS, Sepulcre J, Yeo BT, Liu H, Schmansky NJ, et al. The Dynamics of Cortical and Hippocampal Atrophy in Alzheimer Disease. Arch Neurol. 2011; 68:1040–8. DOI: 10.1001/archneurol.2011.167 [PubMed: 21825241]
20. Kim Y, Cho H, Kim Y. Apolipoprotein E4 affects topographical changes in hippocampal and cortical atrophy in Alzheimer's disease dementia: A five-year longitudinal study. J Alheimers Dis. 2015; 44:1075–85.
21. Wolz R, Julkunen V, Koikkalainen J. Multi-method analysis of MRI images in early diagnostics of Alzheimer's disease. PLoS One. 2011; 6e:25446.
22. McDonald C, Gharapetian, McEvoy L. Relationship between regional atrophy rates and cognitive decline in mild cognitive impairment. Neurobiol Aging. 2012:242–53. [PubMed: 20471718]
23. Nagesh V, Tsien CI, Chenevert TL, Ross BD, Lawrence TS, Junick L, et al. Radiation-Induced Changes in Normal-Appearing White Matter in Patients With Cerebral Tumors: A Diffusion Tensor Imaging Study. Int J Radiat Oncol Biol Phys. 2008; 70:1002–10. DOI: 10.1016/j.ijrobp.2007.08.020 [PubMed: 18313524]
24. Chang Z, Kirkpatrick JP, Wang Z, Cai J, Adamson J, Yin F-F. Evaluating Radiation-induced White Matter Changes in Patients Treated with Stereotactic Radiosurgery Using Diffusion Tensor Imaging: A Pilot Study. Technol Cancer Res Treat. 2014; 13:21–8. DOI: 10.7785/tcrt.2012.500358 [PubMed: 23862743]
25. Connor M, Karunamuni R, McDonald C, White N, Pettersson N, Moiseenko V, et al. Dose-dependent white matter damage after brain radiotherapy. Radiother Oncol. 2016; 121:209–16. DOI: 10.1016/j.radonc.2016.10.003 [PubMed: 27776747]
26. Mabbott DJ, Noseworthy MD, Bouffet E, Rockel C. Diffusion tensor imaging after cranial radiation in children for medulloblastoma: Correlation with IQ. 2006; :244–52. DOI: 10.1215/15228517-2006-002
27. Chapman C, Nagesh V, Sundgren P, Buchtel H, Chenevert T, Junck L, et al. Diffusion tensor imaging of normal-appearing white matter as biomarker for radiation-induced late delayed cognitive decline. Int J Radiat Oncol Biol Phys. 2012; 82:2033–40. [PubMed: 21570218]
28. Kazda T, Jancalek R, Pospisil P, Sevela O, Prochazka T, Vrzal M, et al. Why and how to spare the hippocampus during brain radiotherapy: the developing role of hippocampal avoidance in cranial radiotherapy. 2014; 9:1–10. DOI: 10.1186/1748-717X-9-139
29. Gondi V, Tomé WA, Mehta MP. Why avoid the hippocampus ? A comprehensive review. Radiother Oncol. 2010; 97:370–6. DOI: 10.1016/j.radonc.2010.09.013 [PubMed: 20970214]
30. Farjam R, Pramanik P, Aryal MP, Srinivasan A, Chapman CH, Tsien CI, et al. A Radiation-Induced Hippocampal Vascular Injury Surrogate Marker Predicts Late Neurocognitive Dysfunction. Radiat Oncol Biol. 2015; 93:908–15. DOI: 10.1016/j.ijrobp.2015.08.014
31. Seibert TM, Karunamuni RA. Radiation dose-dependent hippocampal atrophy detected with longitudinal volumetric magnetic resonance imaging. Int J Radiat Oncol Biol Phys. 2016; 97:263–9. [PubMed: 28068234]
32. Karunamuni RA, Moore KL, Seibert TM, Li N, White NS, Bartsch H, et al. Radiation sparing of cerebral cortex in brain tumor patients using quantitative neuroimaging. Radiother Oncol. 2016; 118:29–34. DOI: 10.1016/j.radonc.2016.01.003 [PubMed: 26806266]
33. RTOG 0825. Phase III double-blind placebo-controlled trial of conventional concurrent chemoradiation and adjuvant temozolomide plus bevacizumab versus conventional concurrent chemoradiation and adjuvant temozolomide in patients with newly diagnosed glioblastoma. 2014
34. Woods K, Nguyen D, Tran A, Yu V, Cao M, Niu T, et al. Viability of non-coplanar VMAT for liver sbrt as compared to coplanar VMAT and beam orientation optimized 4pi IMRT. Adv Radiat Oncol. 2016; 1:67–76. [PubMed: 27104216]
35. Nguyen D, Thomas D, Cao M, O'Connor D, Lamb J, Sheng K. Computerized triplet beam orientation optimization for mri-guided co-60 radiotherapy. Med Phys. 2016; 43
36. Niemierko A. A generalized concept of equivalent uniform dose (EUD). Med Phys. 1999; 26:1100.

Author Manuscript Author Manuscript Author Manuscript Author Manuscript

37. Oinam A, Singh L, Shukla A, Ghoshal S, Kapoor R, Sharma S. Dose volume histogram analysis and comparison of different radiobiological models using in-house developed software. J Med Phys. 2011; 36:220–9. [PubMed: 22228931]

38. Feuvret L, Noel G, Mazeron J, Bey P. Conformity index: A Review. Int J Radiat Oncol Biol Phys. 2006; 64:333–42. [PubMed: 16414369]

39. Kataria T, Sharma K, Subramani V, Karrthick K, Bisht S. Homogeneity index: An objective tool for assessment of conformal radiation treatments. J Med Phys. 2012; 37:207–13. [PubMed: 23293452]

40. Qiu D, Leung L, Kwong D, Chan G, Khong P. Mapping radiation dose distribution on the fractional anisotropy map: Applications in the assessment of treatment-induced white matter injury. Neuroimage. 2006; 31:109–15. [PubMed: 16448821]

41. Gondi V, Pugh SL, Tome WA, Caine C, Corn B, Kanner A, et al. Preservation of memory with conformal avoidance of the hippocampal neural stem-cell compartment during whole-brain radiotherapy for brain metastases (RTOG 0933): A phase II multi-institutional trial. J Clin Oncol. 2014; 32:3810–6. DOI: 10.1200/JCO.2014.57.2909 [PubMed: 25349290]

42. Nguyen D, Rwigema JM, Yu VY, Kaprealian T, Kupelian P, Selch M, et al. Feasibility of extreme dose escalation for glioblastoma multiforme using 4 π radiotherapy Feasibility of extreme dose escalation for glioblastoma multiforme using 4 π radiotherapy. 2014; :1–8. DOI: 10.1186/s13014-014-0239-x

43. Nguyen D, Dong P, Long T, Ruan D, Low D, Romeijn E, et al. Integral dose investigation of non-coplanar treatment beam geometries in radiotherapy. Med Phys. 2014; 41:11905.

44. Dong P, Nguyen D, Ruan D, King C, Long T, Romeijn E, et al. Feasibility of prostate robotic radiation therapy on conventional c-arm linacs. Pr Radiat Oncol. 2014; 4:254–60.

45. Yu V, Tran A, Nguyen D, Cao M, Ruan D, Low D, et al. The development and verification of a highly accurate collision prediction model for automated noncoplanar plan delivery. Med Phys. 2015; 42:6457–67. [PubMed: 26520735]

Author Manuscript Author Manuscript Author Manuscript Author Manuscript

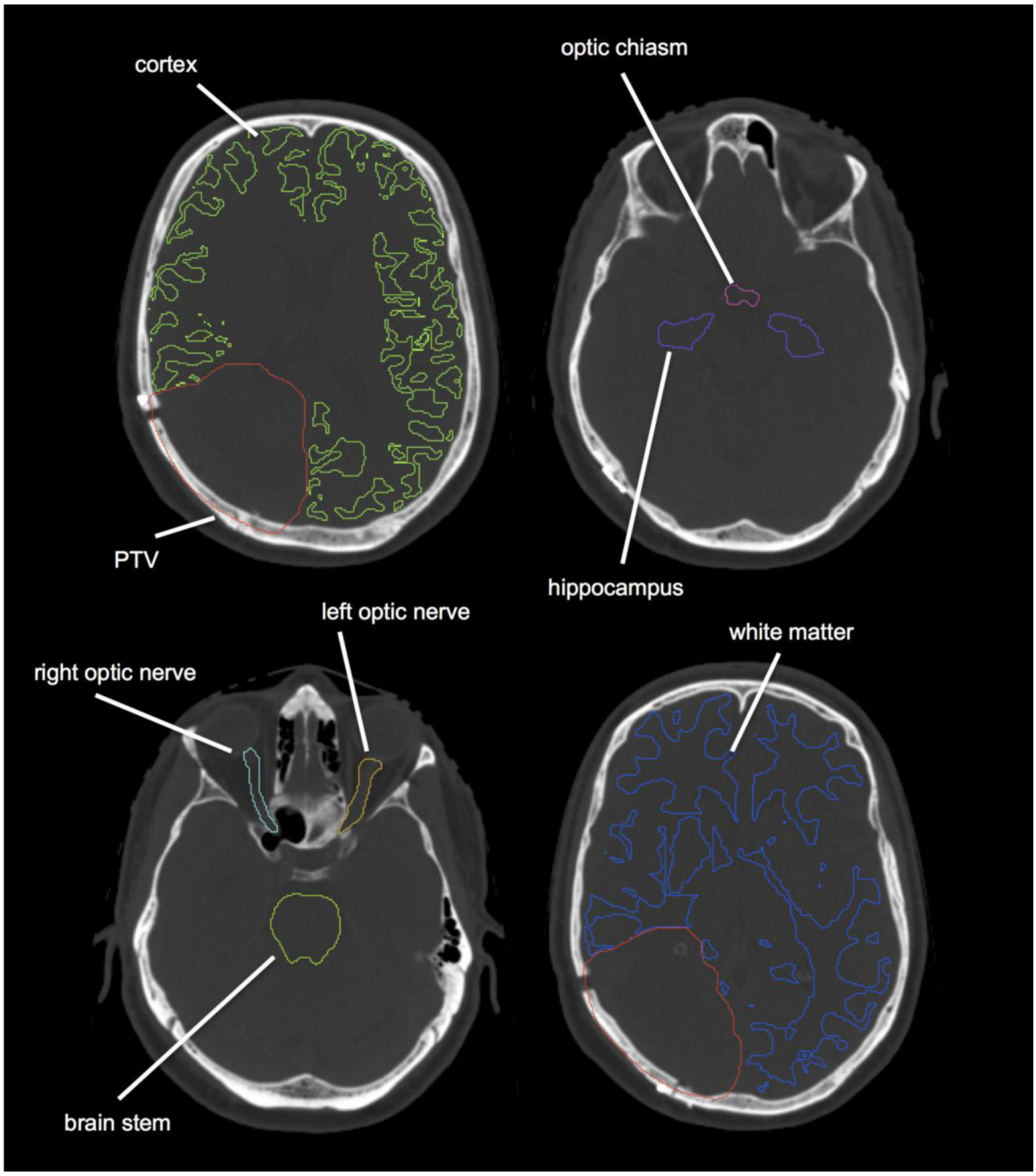

Fig. 1.

Axial images of a representative case showing planning target volume (PTV), cerebral cortex and other organs at risk (OARs) used for planning (brainstem, hippocampus, optic nerves and optic chiasm).

Author Manuscript Author Manuscript Author Manuscript Author Manuscript

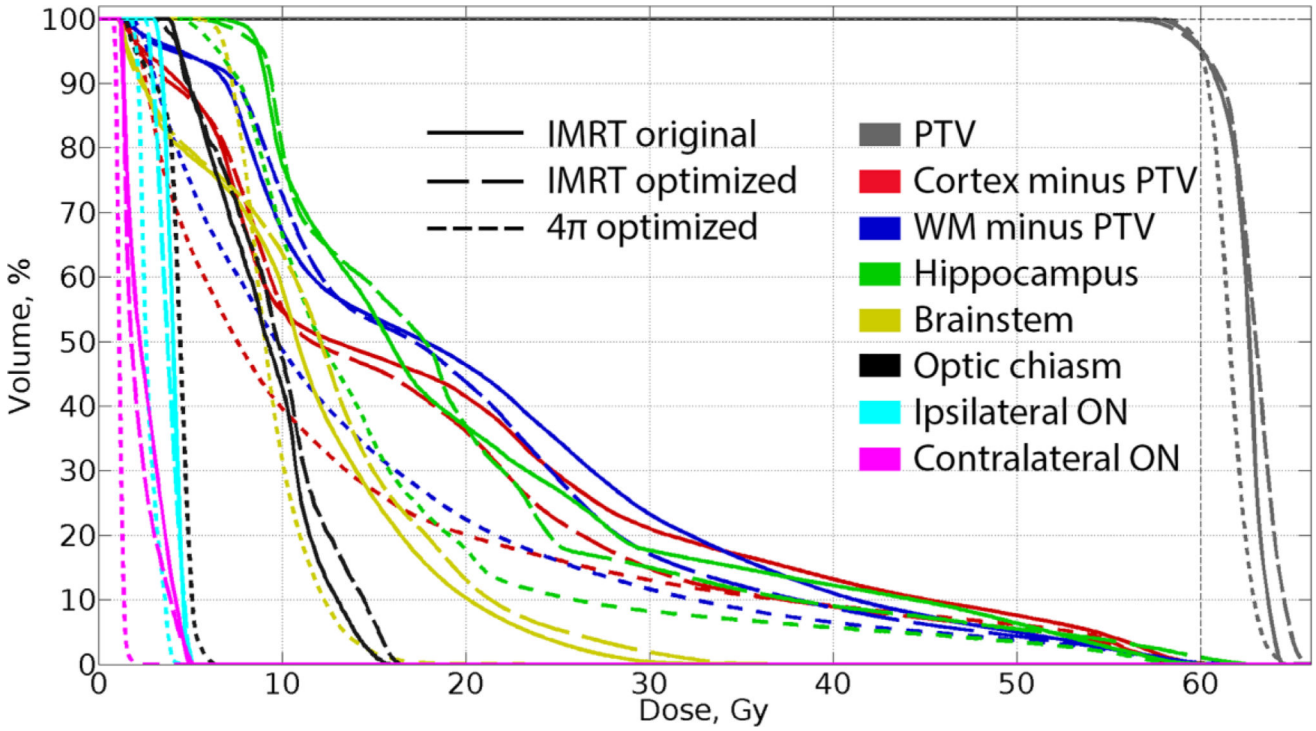

Fig. 2.

Dose-volume histogram for a representative patient. 4π optimized plan (short dashed line) allows for better sparing of all OARs, subcortical white matter and normal cortex.

Author Manuscript
Author Manuscript
Author Manuscript
Author Manuscript

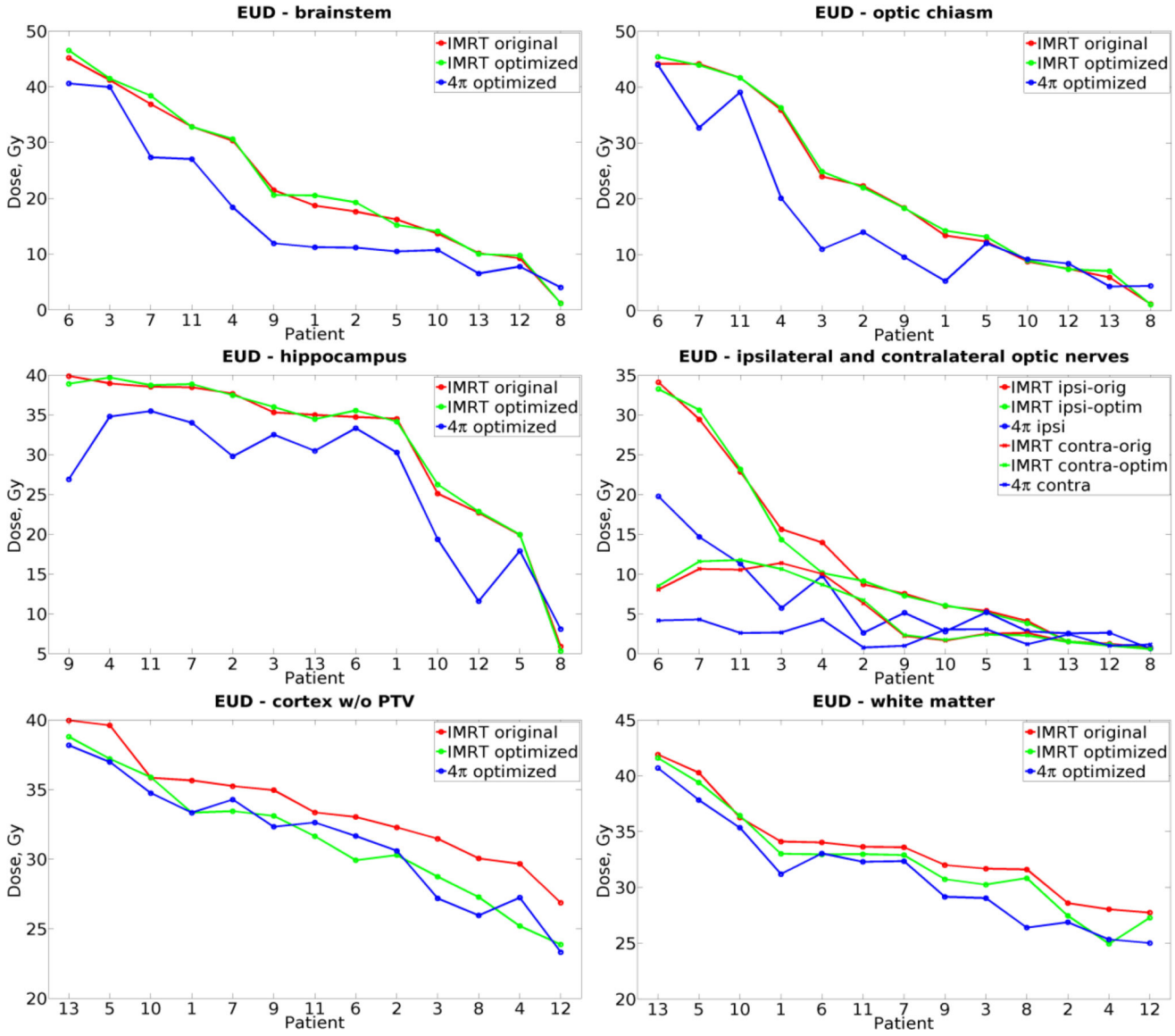

Fig. 3.

Equivalent uniform dose (EUD) calculated from original clinical IMRT (red), plans optimized for brain sparing (green) and corresponding 4π optimized plans (blue) for cortex minus PTV, white matter and OARs: optic nerves, chiasm, brainstem and hippocampus. Patients are sorted in descending order of original IMRT EUD.

Author Manuscript Author Manuscript Author Manuscript Author Manuscript

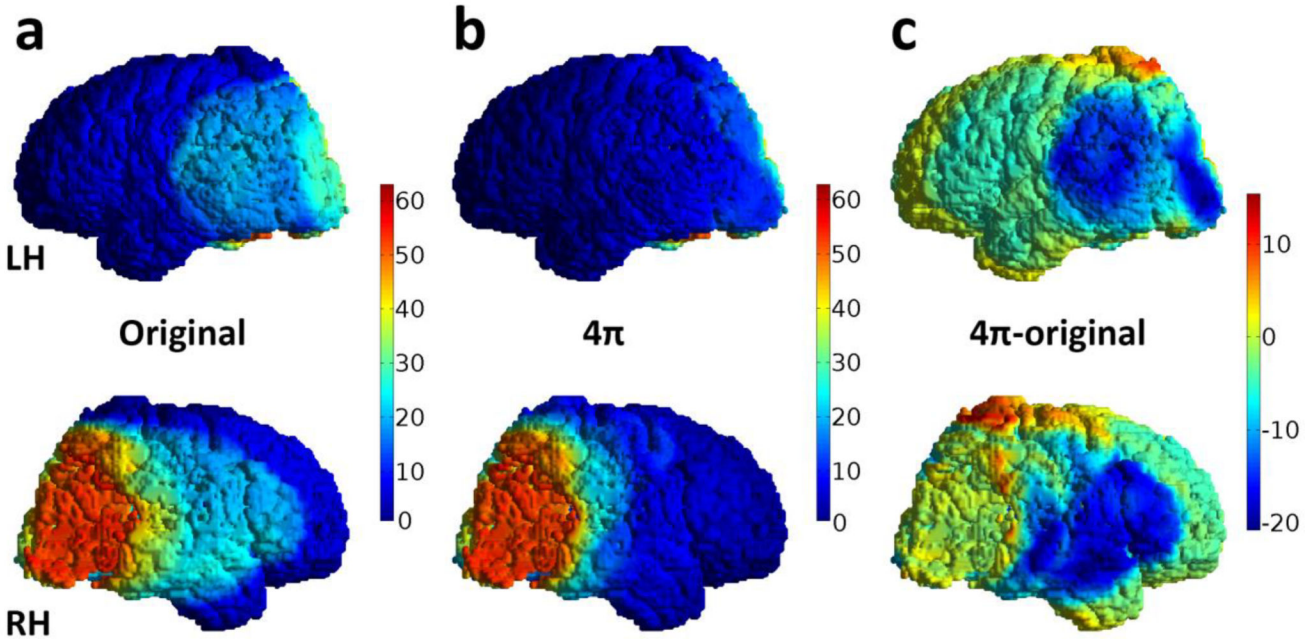

Fig. 4.

Illustrative dose maps on the cortical surface of the subject from Figure 1 (top row – left hemisphere (LH), bottom row – right hemisphere (RH)) a) original plan, b) 4π optimized plan and c) the absolute difference (4π – original). Dose reduction is as great as −20 Gy in some areas, but small non-coplanar volumes (red hot spots) received greater doses than the nearly zero dose in the coplanar plans.

Author Manuscript Author Manuscript Author Manuscript Author Manuscript

Table 1

Dosimetric comparison of original IMRT, optimized IMRT, and 4π optimized plans:

Variable		IMRT original median (range)	IMRT optimized median (range)	4π optimized median (range)	4π-IMRT orig % diff (p-value)	4π-IMRT opt % diff (p-value)
Conformity index		1.00(0.97–1.31)	1.02(1.00–1.29)	1.03(0.99–1.30)	2%(0.001)*	0%(0.414)
Homogeneity index (%)		7.95(4.35–9.29)	9.78(5.45–12.38)	7.11(4.90–10.13)	−11%(0.839)	−27%(0.005)*
Gradient measure (cm)		2.01(1.13–2.59)	1.75(0.97–2.33)	1.60(0.72–2.12)	−20%(<0.001)*	−8%(0.001)*
Max point dose PTV (Gy)		64.7(62.6–68.1)	66.4(63.6–74.7)	66.2(64.1–68.6)	2%(0.017)	0%(0.685)
Min point dose PTV (Gy)		55.1(24.1–57.2)	52.6(20.6–57.1)	55.7(46.5–57.6)	1%(0.273)	6%(0.010)
Brainstem	D_{max} (Gy)†	32.8(1.8–58.9)	35.3(1.7–59.8)	21.7(8.3–59.6)	−34%(0.006)	−38%(0.005)*
	D_{mean} (Gy)	11.4(0.9–39.4)	12.3(0.9–41.4)	8.2(2.0–22.6)	−28%(0.017)	−33%(0.017)
	EUD (Gy)	18.7(1.2–45.1)	20.5(1.1–46.5)	11.2(4.0–40.6)	−40%(0.001)*	−45%(0.001)*
Optic chiasm	D_{max} (Gy)	21.3(1.3–52.1)	21.8(1.2–54.3)	13.0(5.2–54.3)	−39%(0.080)	−40%(0.022)
	D_{mean} (Gy)	14.0(1.1–33.2)	12.0(1.1–31.6)	8.2(2.2–22.4)	−41%(0.022)	−32%(0.008)
	EUD (Gy)	18.4(1.2–44.2)	18.3(1.1–45.4)	11.0(4.3–43.9)	−40%(0.027)	−40%(0.010)
Ipsilateral optic nerve	D_{max} (Gy)	9.9(1.0–52.0)	10.1(0.9–53.4)	7.6(1.0–45.8)	−23%(0.048)	−25%(0.048)
	D_{mean} (Gy)	7.6(0.8–34.1)	7.3(0.7–33.2)	5.2(0.7–19.8)	−32%(0.006)	−29%(0.013)
	EUD (Gy)	8.4(0.9–44.2)	8.4(0.8–44.9)	6.5(0.9–36.8)	−23%(0.027)	−23%(0.009)
Contralateral optic nerve	D_{max} (Gy)	6.5(1.0–23.5)	6.6(0.9–24.6)	4.9(1.0–13.5)	−25%(0.048)	−26%(0.040)
	D_{mean} (Gy)	2.6(0.8–11.4)	2.4(0.7–11.8)	2.6(0.7–4.3)	−1%(0.033)	9%(0.040)
	EUD (Gy)	5.5(0.9–19.9)	5.5(0.8–21.1)	4.0(0.9–10.6)	−27%(0.040)	−28%(0.007)
Hippocampus	D_{max} (Gy)	60.1(19.9–61.8)	61.4(17.0–62.8)	58.3(22.1–63.3)	−3%(0.893)	−5%(0.048)
	D_{mean} (Gy)	20.1(1.9–28.2)	20.1(1.7–29.2)	12.4(6.1–16.2)	−38%(0.002)*	−39%(0.005)*
	EUD (Gy)	35.0(5.9–39.9)	35.5(5.3–39.7)	30.3(8.1–35.5)	−14%(0.001)*	−15%(0.003)*
Cortex minus PTV	D_{max} (Gy)	61.4(60.8–63.4)	62.8(60.9–65.5)	63.0(61.3–64.4)	3%(<0.001)*	0%(0.340)
	D_{mean} (Gy)	14.5(9.0–23.9)	13.0(7.9–21.6)	10.9(6.7–20.5)	−25%(<0.001)*	−16%(<0.001)*

Author Manuscript Author Manuscript Author Manuscript Author Manuscript

Variable		IMRT original median (range)	IMRT optimized median (range)	4π optimized median (range)	4π-IMRT orig % diff (p-value)	4π-IMRT opt % diff (p-value)
	EUD (Gy)	33.3(26.9–40.0)	31.6(23.9–38.8)	32.3(23.3–38.2)	−3%(<0.001) *	2%(0.946)
	V_{60}	0.09(0.02–0.63)	0.06(0.01–0.26)	0.16(0.01–0.53)	76%(0.414)	160%(0.080)
	V_{50}	6.30(1.57–16.41)	4.91(0.77–13.97)	5.60(0.82–13.43)	−11%(<0.001) *	14%(0.340)
	V_{40}	8.63(3.40–22.81)	6.72(1.99–19.39)	7.55(1.74–17.73)	−13%(<0.001) *	12%(0.340)
	V_{30}	15.81(6.72–33.77)	10.59(4.20–26.78)	9.85(2.99–22.09)	−38%(<0.001) *	−7%(0.008)
	D_{max} (Gy)	60.1(19.9–61.8)	61.4(17.0–62.8)	58.3(22.1–63.3)	−3%(0.893)	−5%(0.048)
	D_{mean} (Gy)	15.9(8.2–28.0)	14.8(6.7–27.3)	12.3(7.4–24.1)	−23%(<0.001) *	−17%(0.001) *
	EUD (Gy)	33.6(27.7–41.9)	32.9(24.9–41.6)	31.2(25.0–40.7)	−7%(<0.001) *	−5%(0.001) *
White matter minus PTV	V_{60}	0.08(0.01–0.88)	0.17(0.02–0.83)	0.14(0.02–0.85)	77%(0.191)	−17%(0.305)
	V_{50}	5.04(1.67–20.02)	4.43(0.99–19.09)	3.86(1.05–18.31)	−23%(<0.001) *	−13%(0.005)
	V_{40}	8.74(4.00–28.77)	7.77(2.12–26.44)	6.55(2.23–21.94)	−25%(<0.001) *	−16%(<0.001) *
	V_{30}	13.93(6.26–40.90)	12.06(4.16–38.01)	9.64(4.21–28.91)	−31%(<0.001) *	−20%(<0.001) *
	>2%	0.44(0.37–0.58)	0.42(0.35–0.55)	0.39(0.33–0.53)	−12%(<0.001) *	−8%(<0.001) *
Cortical thinning	>3%	0.26(0.18–0.40)	0.24(0.16–0.36)	0.20(0.14–0.34)	−21%(<0.001) *	−14%(<0.001) *
	>5%	0.12(0.06–0.25)	0.09(0.04–0.22)	0.09(0.04–0.19)	−26%(<0.001) *	−3%(0.001) *

*statistically significant p-values after Bonferroni correction (p<0.005)

†Dose at volume of 0.03cc per RTOG 0825 [33]. All other max doses are maximum point dose to the respective structure.